

Review Article

Cell response of anodized nanotubes on titanium and titanium alloys

Sepideh Minagar,¹ James Wang,¹ Christopher C. Berndt,¹ Elena P. Ivanova,² Cuie Wen¹

¹IRIS, Faculty of Engineering and Industrial Sciences, Swinburne University of Technology, Hawthorn, Victoria 3122, Australia

²Faculty of Life and Social Sciences, Swinburne University of Technology, Hawthorn, Victoria 3122, Australia

Received 24 October 2012; accepted 21 December 2012

Published online 21 February 2013 in Wiley Online Library (wileyonlinelibrary.com). DOI: 10.1002/jbm.a.34575

Abstract: Titanium and titanium alloy implants that have been demonstrated to be more biocompatible than other metallic implant materials, such as Co–Cr alloys and stainless steels, must also be accepted by bone cells, bonding with and growing on them to prevent loosening. Highly ordered nanoporous arrays of titanium dioxide that form on titanium surface by anodic oxidation are receiving increasing research interest due to their effectiveness in promoting osseointegration. The response of bone cells to implant materials depends on the topography, physicochemistry, mechanics, and electronics of the implant surface and this influences cell behavior, such as adhesion, proliferation, shape, migration, survival, and differentiation; for example the existing anions on the surface of a titanium implant make it negative and this affects the interaction with negative fibronectin (FN). Although optimal nanosize of reproducible titania nanotubes

has not been reported due to different protocols used in studies, cell response was more sensitive to titania nanotubes with nanometer diameter and interspace. By annealing, amorphous TiO₂ nanotubes change to a crystalline form and become more hydrophilic, resulting in an encouraging effect on cell behavior. The crystalline size and thickness of the bone-like apatite that forms on the titania nanotubes after implantation are also affected by the diameter and shape. This review describes how changes in nanotube morphologies, such as the tube diameter, the thickness of the nanotube layer, and the crystalline structure, influence the response of cells. © 2013 Wiley Periodicals, Inc. *J Biomed Mater Res Part A*: 101A: 2726–2739, 2013.

Key Words: titanium implants, anodization, TiO₂ nanotubes, cell response, osteoblast

How to cite this article: Minagar S, Wang J, Berndt CC, Ivanova EP, Wen C. 2013. Cell response of anodized nanotubes on titanium and titanium alloys—A review. *J Biomed Mater Res Part A* 2013;101A:2726–2739.

INTRODUCTION

Among different biomaterial implants used for implants, such as ceramics, polymers, composites and natural products, metal implants are preferred for load-bearing applications because they exhibit excellent mechanical properties such as Young's modulus, tensile strength, ductility, fatigue life, and wear resistance¹ in addition to chemical properties such as corrosion resistance, biocompatibility and the ability to fuse and harmonize with other implant materials.² These properties make them more suitable for long-term use in hard tissue applications such as hip and knee joints.^{2,3} Stainless steels and cobalt–chromium–molybdenum alloys are examples alongside more biocompatible titanium and titanium alloys.⁴ Biomaterials have progressed through three generations from the first, whose particularities were matching its physical properties as a tissue replacement

with the least toxicity or biological inertness to the second generation that demonstrate bioactive behavior.⁵ Surface treatments have been used to improve the bioactive nature of these biomaterials, especially metals such as titanium and titanium alloys that change the physicochemical, mechanical, and electrical properties of their surfaces.⁶ The third generation biomaterials are intended to promote specific cellular responses at the molecular level.⁵ The significance of surface treatment such as anodic oxidation⁷ that provides the possibility of controlled nanoscale fabrication with suitable physicochemical properties on the metal surface has been reported.⁸ Such nanoscale surfaces exhibit similar properties to those of physiological bone. Table I lists the size scales of the hierarchical bone components, in comparison to the size scales of the implant structures. Factors important to cell response can be better controlled by

Correspondence to: C. Wen; e-mail: cwen@swin.edu.au

Contract grant sponsor: State Government of Victoria in Australia through the Victorian International Research Scholarship (SM)

Contract grant sponsor: Australian Research Council (ARC) through the ARC Discovery Project; contract grant number: DP110101974 (CW)

TABLE I. Scale of Sizes of the Hierarchical Bone Components, in Comparison to the Scale Sizes of the Implant Structures

Structures	Size		Ref.
	Micrometer	Nanometer	
<i>Tissue component</i>			
Osteon	10–500	–	80
Osteoclast (lacunae)	100 or more	–	88
Osteoblast	20–30	–	88
Lamella	3–7	–	80
Collagen fibril	0.5	–	80
Cell membrane	–	10–100	89
Plate-like apatite crystals	–	50 × 25 × 3	80
Integrins	–	8–12	87
Proteins	–	1–10	89
Collagen molecule	–	1	80
Amino acids	–	0.1–1	89
Water molecule	–	0.1	89
<i>Metal implant</i>			
Roughness of the surface	>100	–	89
titanium grain sizes	10–20	–	66
Metal oxide	–	5–15	89
Atom	–	0.1	89

understanding the mechanism of cell attachment to the biomaterial surface.

Various populations of cells, cytokines, growth factors, and extracellular matrix (ECM) affect the process of tissue healing around implants. For example, chemotactic factors are essential for cell recruitment and cell adhesion, and growth factors and cytokines are effective for the proliferation and differentiation of cells. Protein adsorption at the implant surface initiates interactions between cells and implants through a complex series of adsorption and displacement steps. The interaction of cell and implant is followed by the attachment phase that is governed mainly by van der Waals forces. The next step, termed the adhesion phase, is surface anchoring through fibronectin (FN) and vitronectin for the formation of focal points at cell membrane integrins. Filopodia and finger-like protrusions are then produced to enable sensing of the optimum anchorage and spreading toward the surface.^{9,10}

Although the effects of TiO₂ nanotube surfaces for bone regeneration and different type of cells have been reviewed recently^{11,12} the current work aimed evaluating the factors that influence cell behavior, followed by highlighting the recent studies of improvement on physicochemical and other properties of TiO₂ nanotubes, and of the bone cells response with regard to enhancing osseointegration.

FACTORS THAT INFLUENCE BONE CELL ADHESION

The ECM secreted by cells plays a role as the interface of a biomaterial surface. ECM is synthesized and degraded by cells as a dynamic surrounding substance that consists of 90% collagenic proteins (type I collagen and type V collagen) and 10% noncollagenic proteins (for example osteocalcin, osteonectin, bone sialoproteins, proteoglycans, osteo-

ponin, FN, growth factors, bone morphogenetic proteins, etc.).¹⁰ Anselme et al.¹³ indicated that the cells are always in contact with a biomaterial surface that has previously adsorbed water and proteins from biological fluids, rather than with a bare surface. Specific receptor proteins such as integrins, as well as the junctions of adherents containing cadherins mediating cell–cell adhesions, are important for cell–substrate adhesion. Focal contacts or adhesion plaques are junction locations of about 10–15 nm where adherent cells and material surfaces are joined. Integrins are on the external side of focal contacts and they can translate the attachment of external ligands to internal information that induces adhesion, spreading, or cell migration, growth and differentiation.¹⁰ It has been shown that the vinculin and paxillin can play an essential role in continuing adhesion and upcoming differentiated cell functions.¹⁴ The cell proteins involved in cell adhesion on biomaterial are illustrated in Figure 1.

The adhesion force at the cell/implant interface determines phenomena that involve short term and long term adhesion due to (i) physicochemical linkages such as ionic forces and van der Waals forces and (ii) different biological molecules such as ECM proteins, cell membrane proteins, and cytoskeleton proteins. The adhesion can be measured using a variety of methods such as micropipettes aspiration, centrifugation (the force necessary to separate cells from a substrate is provided by centrifugal force),¹⁵ and fluid flow; enzymatic procedures; optical or magnetic tweezers (measure local viscoelastic properties of the surface of adhering cell by a magnetic bead microrheometer¹⁶); and microcantilevers (detaching adhered cell by applying a lateral load using a microcantilever and measuring the detachment force¹⁷) for the detachment of cell populations by micromanipulation.¹³ By micropipettes aspiration, the strength of cell adhesion can be measured by vertically oscillating micropipette while it makes contact with cell and the pressure within the micropipette is reduced to a level that cell can attach to the pipette by suction.¹⁸ Glass, silane-adherent cells¹⁹ deposited in glass and silane capillary tubes can be detached by calibrated laminar shear flows with a highly viscous dextran solution. This method is known as fluid flow.²⁰

There are different opinions concerning the preferred bone growth direction around implants, for example, toward the implant, on the implant surface, or both together.^{13,21} In addition to the cell type, the surface chemistry, mechanical cues, and topography influence cell behaviors such as adhesion, proliferation, shape, migration, survival, and differentiation.^{13,21,22} It has also been reported that there are different mechanisms of adhesion for blood cells, fibroblasts or osteoblasts (connective tissues), and endothelial vascular cells or keratinocytes (endothelia or epithelia), such as adherence and proliferation rate.¹³

The influence of surface physicochemical, mechanical and electrical properties on bone cell behavior

Surface chemistry plays an important role in the cell response at interfaces. The effect of surface energy, water contact angle or wettability (hydrophilicity and

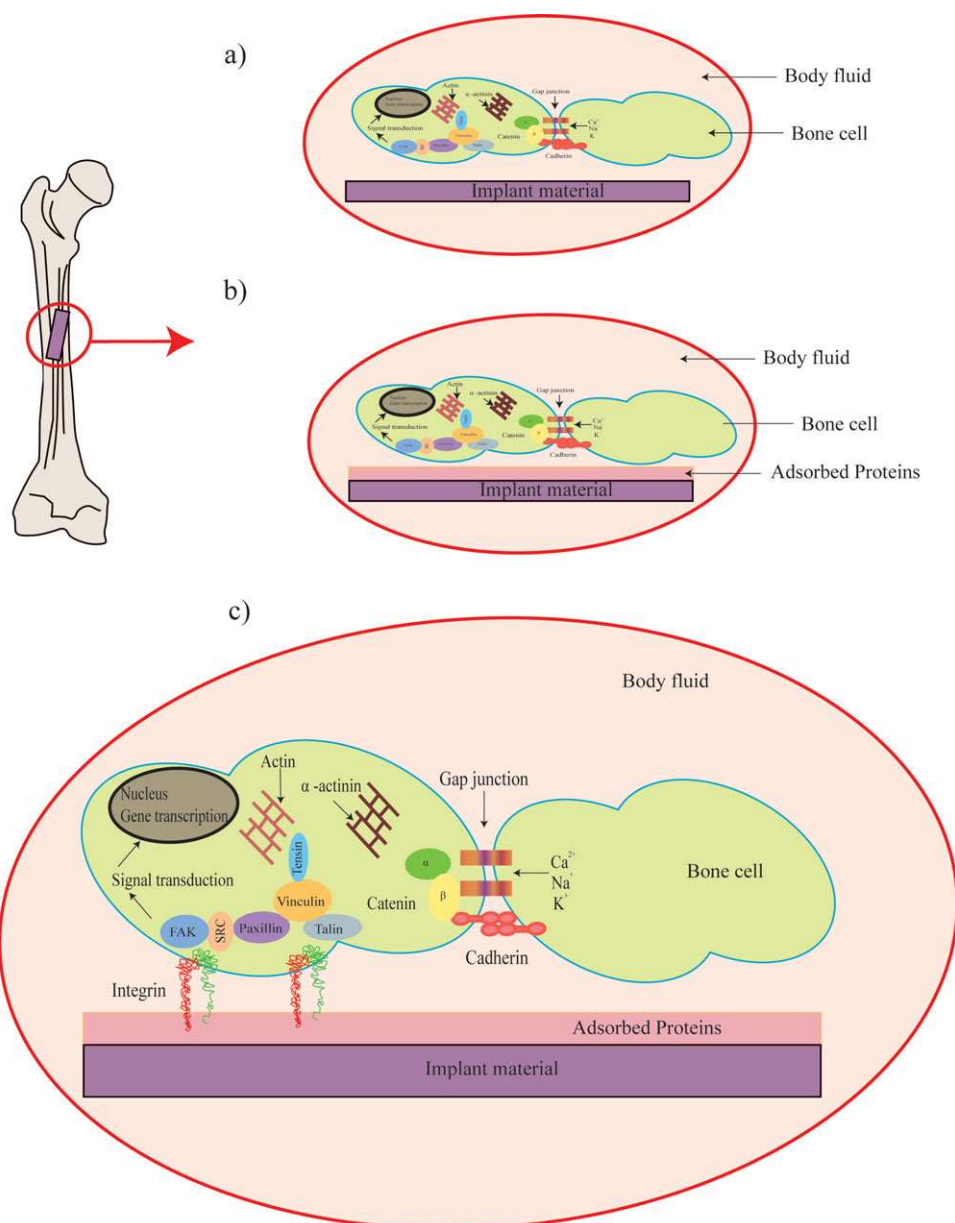


FIGURE 1. Representation of the cell proteins involved in cell adhesion on biomaterial: (a) immediately after implantation; (b) adsorbing proteins from body fluid; and (c) attached bone cell on an implant material surface in higher magnification (Adapted from Ref. 10, with permission from Biomaterials). [Color figure can be viewed in the online issue, which is available at wileyonlinelibrary.com.]

hydrophobicity), and the zeta potential of different surfaces on cell behavior have been reviewed.¹³ Protein adsorption, cell adhesion, proliferation, and osteoblastic differentiation will be increased by a decrease in the water contact angle or an increase in surface energy. Electrical charges on titanium surfaces that are measured as zeta potential are important in the interaction with negatively charged proteins such as FN.^{9,23} A titanium surface, normally, is negatively charged due to the adsorption of anions (OH^- , F^- , etc. from the electrolyte). On the other hand, cell membranes are also negatively charged, so positively charged proteins at the cell surface interface can play an important role, which is proposed as a dynamic model for osteoblast attachment.²³ The

adhesion constant and binding efficiency of adsorbed proteins on different functional groups (e.g., OH , COOH , NH_2 , and CH_3) demonstrate different adhesion strengths.⁹

Changing the surface topography to nanoscale does not change the surface chemistry with respect to its bulk, but it might change the surface chemistry and energy at the interface. Rising hydrophobicity is one example of the influence of surface density on surface chemistry. Decuzzi and Ferrari²⁴ proposed a mathematical model and introduced three regimes for surface energy including small, intermediate and large. They then investigated the effects of surface roughness on cell adhesion in these three regimes, and found that cell adhesion will deteriorate with an increase in

roughness for small energy surfaces, exhibit maximum adhesion for an optimal roughness yet will be scarcely affected by roughness for intermediate surface energies.²⁴ In the line of the above mentioned model, stable cell adhesion and proliferation for four different cell lines have been reported to be increased on moderately rough Brownian substrates with nearly similar surface energy but the generality of the results need additional studies to verify.²⁵

Osteoprecursor cell line attachment and growth behavior on TiO₂ nanotubes with ~50 nm diameter were also studied.²⁶ The effects of the physicochemical properties of the surface, for instance, roughness, contact angle, and surface energy, on the cell behavior were investigated and it was found that materials with a high nanoscale roughness, low contact angle, and high surface energy showed the same positive effect on cell behavior, such as early differentiation and significant bone cell proliferation, which means an improvement in cell adhesion and spreading.²⁶ Kim et al.²⁷ indicated that cell behavior is affected by the incorporated anions in the oxide layer rather than the morphology of surface. It was shown that the composition of the electrolyte, for example HF, HF+H₃PO₄, and H₃PO₄ not only determines the oxide morphologies (dot-like structures, granules, nanopowders, and nanotubes), but it also affects the incorporation levels of the ions of F⁻ and PO₄³⁻, which cause different cell behaviors: the PO₄³⁻ enriched oxides enhance cell proliferation in 7 days and the F⁻ enriched oxides stimulate initial cell attachment.²⁷

Mechanical cues, for instance, rigidity, stiffness, and resilience, have been shown to influence cell behavior.¹³ Influence of microenvironment stiffness on stem cell specifications has been observed when the cells commit to the lineage specified by matrix elasticity after several weeks in culture in inverse to the initial week in culture that could be reprogrammed these lineages by adding soluble induction factors.²⁸ Mechanical feedback regarding substrate rigidity is essential for the cell to shape, grow, and survive, but recognition by the cells of their microenvironment and elasticity and its influence on the structure and function of the cells is still under investigation.^{13,29-31}

Effect of topography on the bone cell behavior

Chen et al.³² reported that a decrease in the surface roughness of Ti resulted in an increase in its corrosion resistance and a decrease in ion release. The roughness of a metallic implant surface and its uniformity in the horizontal or vertical direction influence its favorable mechanical locking to tissues. Several hypotheses regarding the mechanisms of cell responses to surface topography were proposed in a review by Anselme et al.³³ ECM protein adsorption acts as an energy barrier for cells to modify their orientation, adhesion and spread. Changes in gene expression and in cellular, cytoskeletal, and focal adhesions were observed in a study on cell behavior on micro- and nanoanisotropic topographies, regardless of the long-term turnover.³³ Although there is an absence of comparable studies, cell operation is motivated when the size is ~10 nm in height or depth,³⁴ and

cell operation is not noticeable when the scale increases to ~100 nm.

The principal aim of all research in this field is to improve the wound healing that accompanied by the promotion of osseointegration. Large macrostructure human bones consist of nanosized organic and mineral phases, such as ions, DNA, proteins, and the viruses in the body. There has been insufficient study concerning the retention of proteins on nanoscale surfaces, because fabrication of nanofeatures or nanosurfaces cannot be easily reproduced. Nevertheless, investigation has shown that the structure and function of absorbed proteins on smaller nanoparticles can be readily retained in comparison to larger nanoparticles, but the details of the adsorption mechanisms are not clear.^{33,35} As cell-substrate adhesion is based on integrins that have nanoscale features, it can be predicted that cells will respond better to nanoscale surfaces. Further research needs to be undertaken to clarify this hypothesis.^{13,36} In general, it has been shown that cells respond to nanosurfaces because the pores, ridges, and fibres of the basement membranes have nanoscale characteristics.³⁷ Figure 2 shows filopodia of SaOs-2 cells on 200 nm deep round concentric grooves and ridges in quartz (reproduced from Anselme et al.³³).

Uniform and controllable nanopatterned surfaces of titanium can be fabricated using electrochemical anodic oxidation, which is an economical, simple, and versatile technique.³⁸ By applying a constant potential to titanium as a working electrode in an electrochemical cell with a platinum counter electrode and a standard reference electrode, then titania nanotubes can be obtained. Different TiO₂ nanotube diameters, wall thicknesses and lengths can be achieved by controlling the condition of the anodizing process, such as the applied potential, current density, anodization time, concentration of fluorine ion and type (aqueous and organic), pH value, and the viscosity of the electrolyte.³⁹ Nanotubes start to grow through the compact oxide layer that are formed during the first step of the process on the surface of titanium as a soluble fluoride complex.⁸

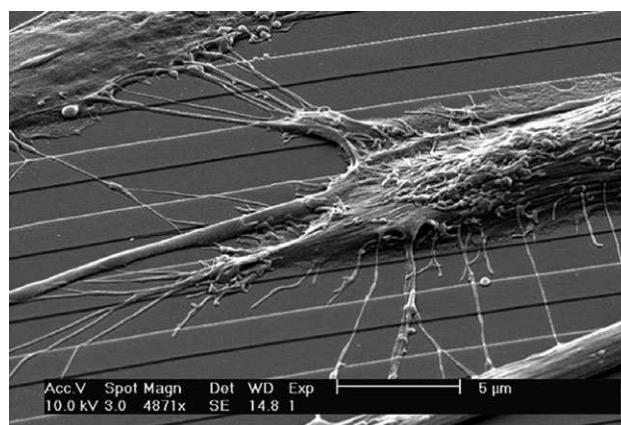


FIGURE 2. SEM image of filopodia of the SaOs-2 cells on 200 nm deep round concentric grooves and ridges in quartz (Reproduced from Ref. 33, with permission from Acta Biomater).

At anode: $\text{Ti} \rightleftharpoons \text{Ti}^{4+} + 4\text{e}^-$ (1)

At cathode: $4\text{H}^+ + 4\text{e}^- \rightleftharpoons 2\text{H}_2$ (2)

In the electrochemical cell: $\text{Ti}^{4+} + 6\text{F}^- \rightleftharpoons [\text{TiF}_6]^{2-}$ (3)

This kind of nanopatterned surface is well suited to an investigation of the mechanism of a bone cell response to the various morphologies of a titanium and titanium alloy surfaces.^{8,40–42} Different TiO_2 nanotubes on the surface of titanium (Ti) and titanium–zirconium (TiZr) alloy, with different nanospacing in aqueous and organic electrolyte, are shown in Figure 3. Nanotubes have been grown by us, as shown in Figure 3(a), with separated walls, were formed in an electrolyte containing 1 M $(\text{NH}_4)_2\text{SO}_4 + 0.3 \text{ wt } \% \text{ NH}_4\text{F}$ on the substrate of a Ti–50 wt % Zr alloy for 1.75 h, exhib-

iting an inner diameter of 14.86 nm and an outer diameter of 30.63 nm. When organic electrolyte of ethylene glycol + 0.5 wt % NH_4F + 2 vol % H_2O was used, the nanotubes displayed nonseparated 7.80 nm thick walls with 15.59 nm nanospacing, 39.11 nm inner diameter, and 10.83 μm length at a longer anodization time of 20 h for Ti–50Zr alloy [Fig. 3(b) and (c)]. Nanotubes with 29.87 nm thick nonseparated walls, 39.32 nm inner diameter, and 1.47 μm length that formed on pure titanium in the presence of 0.1 wt % NH_4F and 1 M $(\text{NH}_4)_2\text{SO}_4$ anodized for 4 h are shown in Figure 3(d) and (e). Figure 3(f) shows that the 60.37 nm bottom diameter nanotubes formed on Ti–50Zr alloy were close at the bottom as they were anodized under the same conditions as Figure 3(b) and (c).

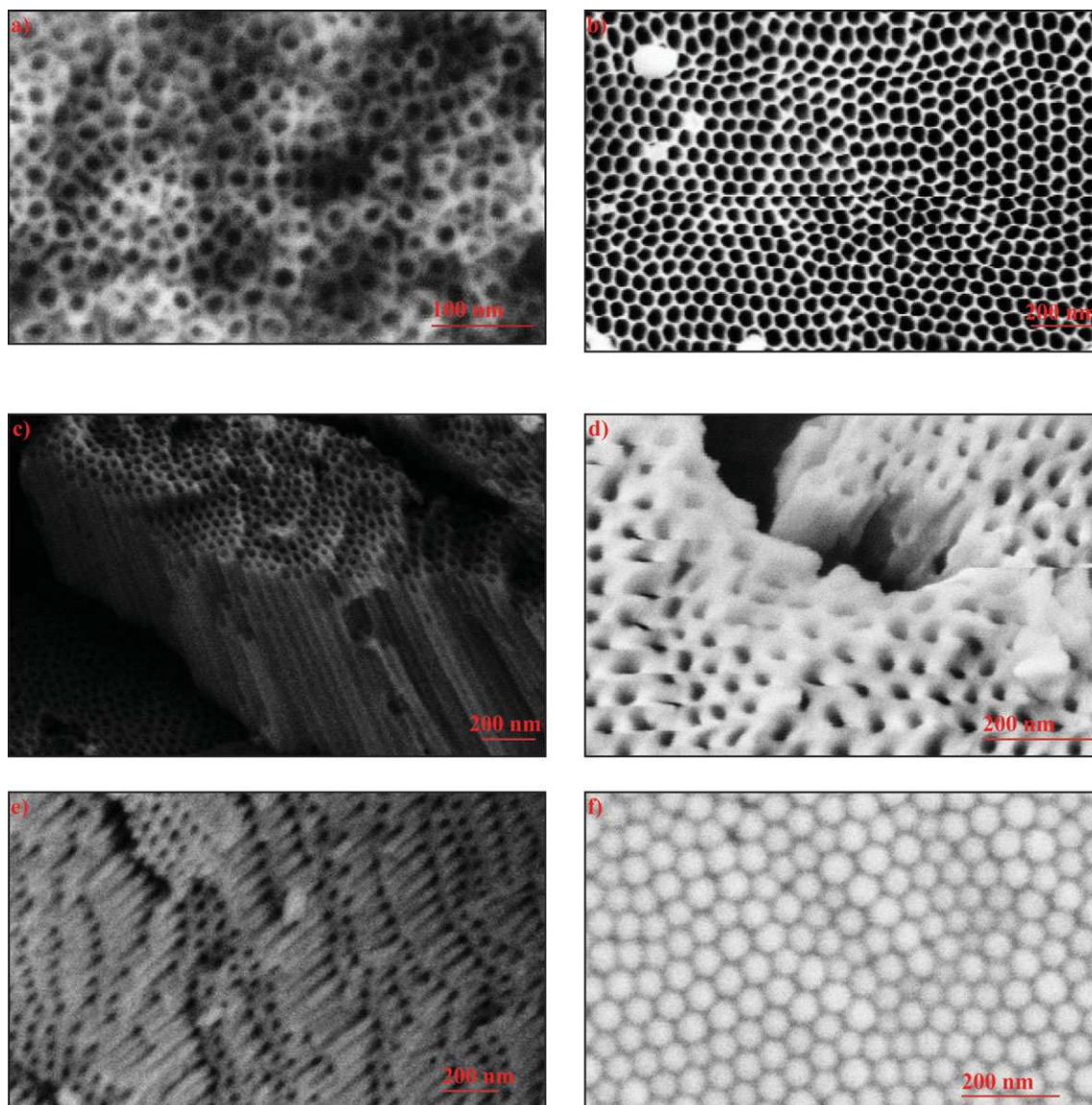


FIGURE 3. SEM images of TiO_2 nanotubes: (a) top view formed in 1 M $(\text{NH}_4)_2\text{SO}_4 + 0.3 \text{ wt } \% \text{ NH}_4\text{F}$ on Ti–50Zr alloy with separated walls, (b) top view formed in ethylene glycol + 0.5 wt % NH_4F + 2 vol % H_2O on Ti–50Zr alloy with nonseparated walls, (c) cross-section formed in ethylene glycol + 0.5 wt % NH_4F + 2 vol % H_2O on Ti–50Zr alloy with nonseparated walls, (d and e) top view and cross-section formed in 1 M $(\text{NH}_4)_2\text{SO}_4 + 0.1 \text{ wt } \% \text{ NH}_4\text{F}$ on CP Ti with nonseparated walls, and (f) bottom view formed in ethylene glycol + 0.5 wt % NH_4F + 2 vol % H_2O on Ti–50Zr alloy. [Color figure can be viewed in the online issue, which is available at wileyonlinelibrary.com.]

In revealing the effect of nanotubular pattern of Ti-30Ta on cell response in comparison to a surface of Ti-30Ta alloy, cellular adhesion, proliferation, viability, cytoskeletal organization and morphology of human dermal fibroblasts (neonatal) were investigated. Nanotube architecture anodized at 35 V for 40 min showed enhancement of improved cellular functionality.⁴³ Good bioactivity for mesenchymal stem cell adhesion and spreading and fast formation of ECM materials on the Ti-Nb-O nanotubes formed on Ti-35Nb has been observed.⁴⁴ There were also some studies on ternary and higher titanium alloys.⁴⁵⁻⁴⁸ Nearly the same cell adhesion rate, the spreading out of attached stem cells, the flat shapes and numerous filopodia after longtime culture occurred for mouse bone marrow mesenchymal stem cells on Ti-35Nb-5Zr in comparison to Ti-35Nb.⁴⁶ Human osteoblast cells growth on anodized nanotubes on Ti-6Al-7Nb in two inorganic and hybrid electrolyte was found to be higher than that of cells cultured on untreated Ti-6Al-7Nb alloy.⁴⁷ The protein adsorption, initial cell adhesion, cell differentiation and osteogenesis related gene expression have been enhanced on sparsely distributed nanotubes on the surface of a near β titanium alloy Ti-5Zr-3Sn-5Mo-15Nb compared to the polished same alloy.⁴⁸

EFFECT OF THE CHARACTERISTICS OF ANODIZED TITANIA NANOTUBES ON BONE CELL BEHAVIOR

The size and distance between nanofeatures on an implant, in addition to adsorbed proteins, as well as the shape or organization of these nanofeatures, influence the cell response.^{33,35} Although there are methods such as lithography and nanoimprinting to fabricate uniform and reproducible nanofeatures on polymeric or other material surfaces, these are not convenient for metals.⁹ Anodic oxidation is a method to tailor nanoscale patterned surfaces for metals and alloys.⁷

Effect of nanospacing of the surface of TiO₂ nanotubes on cell behavior

Park et al.⁴⁹ evaluated the adhesion, spreading, growth, and differentiation of rat mesenchymal stem cells on the surface of TiO₂ nanotubes of 15, 20, 30, 50, 70, and 100 nm diameters. Cells were found to adhere and spread widely on 15 nm tubes but the adhesion decreased with an increase in the nanotube diameter. Focal contact formation on nanotubes with a diameter ≤ 30 nm was higher than on those with larger diameters. The cell proliferation rate decreased as the diameter of the nanotubes increased. The highest cell differentiation was also observed on 15 nm tubes. This result was compared with polished TiO₂ surfaces, which showed that the 15 nm tubes offered optimal spacing for cell proliferation, migration, and differentiation resulting from integrin clustering and focal contact formation. Peri-implant bone formation of commercial Ti covered by 30 nm TiO₂ nanotubes was investigated *in vivo* in pigs and it was found that the nanostructures not only promoted osteoblast formation in the initial step but also resisted implant insertion shear force.⁵⁰ Osteoblasts and osteoclasts, which are

responsible for the formation and resorption of bone cells, demonstrated the same reaction to the one-dimensional surface nanotopography of 15 nm TiO₂ nanotubes,⁵¹ even though it is well known that their activities are different due to their different working mechanisms. It has been claimed that the essential nanosize of TiO₂ nanotubes is <100 nm and the best diameter is 15 nm for adhesion and differentiation of various cells.⁵¹

Although MC3T3-E1 mouse osteoblast cells promoted higher adhesion on ~ 30 nm TiO₂ nanotubes, increased elongation of the cells and enhanced alkaline phosphatase (ALP) activity were observed on nanotubes of greater diameter between 70 and 100 nm that are known to have greater bone forming ability.⁵² This conclusion is different from the results reported by Park et al.,⁵¹ in which the optimal diameter of nanotubes is 15 nm. However, the increase in the bone forming ability of a nanotube of ~ 100 nm diameter was caused by crystallization of the nanotube during heat treatment.^{52,53} The adhesion was accelerated by ~ 300 – 400% increase in the number of the adhered cells due to its significantly increased surface area and the presence of fluid between annealed nanotubes or those soaked in sodium hydroxide.^{54,55} The optimum size of a TiO₂ nanotube for osteoconductivity and osseointegration ability has been reported as 70 nm after assessments using an *in vivo* real-time polymerase chain reaction technique, fluorochrome labels and histological analysis,⁵⁶ but this is not completely consistent with the studies mentioned above. Also in a study of the relationship between Zr content and nanotube diameter in the Ti-xZr ($x = 10, 20, 30, 40$) and Ti-30Ta-xZr ($x = 3, 7, 15$) alloy, it has been reported that when Zr content increased nanotube diameter decreased from 200 to 150 nm for Ti-xZr alloy and it decreased from 200 to 50 nm for the ternary alloys. Good MC3T3-E1 mouse osteoblast cell proliferation, migration and differentiation have been observed on the 50 nm diameter of nanotubes formed on the surface of Ti-30Ta-15Zr, better than on Ti alloy with low Zr content.⁴⁵ Although titania nanotubes formed on α phase and β phase of the titanium alloys due to the content of alloying elements⁴⁵ were self-organized, irregular^{47,57} and showed different diameters⁵⁸ which affected the hydroxyapatite (HA) formation⁵⁹ there is still few study on the cell behavior to different phases.

In summary, cells respond to the topography, physicochemistry, and electrical and mechanical properties of the implant surface. They can recognize the topography from a few nanometers to several hundred micrometers following different chemical treatments, especially anodic oxidation where the nanotube layer is reproducible and can be fabricated in a cost effective way. Table II lists the different cell responses to various TiO₂ nanotubes on titanium and the anodization condition from different studies, to date. The interaction between the cells and the TiO₂ nanotubes provides the possibility of controlling the cell culture by ordering the physicochemical properties of the surface. Figure 4 schematically illustrates a bone cell attached to titania nanotubes showing a hypothetical model of adhesion.

TABLE II. Cell Responses to Different TiO₂ Nanotubes on Titanium and the Anodization Conditions

Nanotube Characteristic					Anodization Conditions					Hydroxyapatite Deposition/Cell Response	Ref.
Nanotube Diameter (nm)\	Wall Thickness (nm)	Nanotube Layer Thickness (nm)	Phase Structure	Other Treatment	Electrolyte	Applied Potential (V)	Time (h)	Others			
51.1	50.58	600	Amorphous	HT to anatase and rutile	H ₂ SO ₄ /NaF/citric acid	20	4	pH = 4.5	Osteoblastic precursor cell line (OPC1)/dense focal contacts Proliferation 0.342 High activity Early differentiation in day 5	26	
>100	–	Short length	–	–	H ₃ PO ₄ /HF	20	1	Stirred (≈180 rpm)	MC3T3-E1 cells/good initial attachment of cells not changed through culturing for 7 days	27	
15–20–30–50	–	–	–	–	H ₃ PO ₄ /HF	1–20	–	–	Rat mesenchymal stem cells/adhesion and spreading, proliferation and differentiation were highest for 15 nm diameter	49	
70–100	–	–	–	–	H ₃ PO ₄ /HF	1–20	–	–	Rat mesenchymal stem cells/adhesion and spreading was impaired without stable extension of filopodia lowest impaired	49	
30–100	–	–	Amorphous	HT to anatase	Acetic acid/HF	5–20	–	–	MC3T3-E1/increasing nanotube diameters led to increased elongation/stretching of cell bodies, increased levels of alkaline phosphatase and greater bone forming ability	52	
30–100	–	–	Amorphous	HT into crystalline phase	Acetic acid/HF	5–20	0.5	–	Human mesenchymal stem cells/promoting adhesion without noticeable differentiation at ~30 nm, eliciting a dramatic stem cell elongation at ~70–100 nm, induced cytoskeletal stress and selective differentiation into osteoblast-like cells	90	
100	–	–	–	–	H ₃ PO ₄ /HF	1–20	1	–	Human primary osteoblasts and osteoclast/15 nm was recognized at least by both	51	
70	15	250	Amorphous	HT to anatase	HF	20	0.5	–	MC3T3-E1/Adhesion increase ~300–400%	54	

TABLE II. (Continued).

Nanotube Characteristic				Anodization Conditions				Hydroxyapatite Deposition/Cell Response	Ref.
Nanotube Diameter (nm)	Wall Thickness (nm)	Nanotube Layer Thickness (nm)	Phase Structure	Other Treatment	Electrolyte	Applied Potential (V)	Time (h)	Others	
80	-	400	-	HT to anatase load with gentamicin	HF	20	0.75	-	91
~70	~15	~250	-	Immersed in NaOH then HT to anatase	HF	20	0.5	-	55
100	19	1000	-	HT to anatase and rutile	NH ₄ H ₂ PO ₄ /NH ₄ F	20	1	Stirred	92

HT: heat treatment.

Effect of crystalline phase of TiO₂ nanotubes on bone cell behavior

TiO₂ nanotubes that were tailored on the surface of titanium using anodic oxidation could be easily removed by a moderate touch. Heat treatment has been used to increase the adhesion of nanotubes to the titanium substrates.⁶⁰ Crystalline structures of titania, such as anatase, rutile, and mixture of both, have been observed after this process, which are dependent on the temperature used.⁶¹ At higher temperatures ($\geq 600^\circ\text{C}$), rutile is the remaining structure along with changes in the shapes of the nanotubes. However, at a lower temperature, for instance 450°C , the growth of anatase crystallites occurs along the length and curvatures of the nanotubes, thus the morphology remains stable.⁶² Loss of fluorine can occur during heat treatment, which in turn affects cell adhesion and proliferation.^{27,63} The stability and hydrophilic properties of TiO₂ nanotubes can also be changed through annealing. The diameter of the titania nanotubes annealed at 500°C for 2 h decreased by 34.43%, the wall thickness of the nanotubes increased by 35.65% for a selected nanotube diameter of 25–40 nm, and the measured contact angle value changed from 73.15° to 17.61° after annealing.⁶⁴ Although heat treatment at different temperatures did not influence the surface roughness of the titania nanotubes, the average roughness of the annealed nanotubes was higher than the as-formed nanotubes.⁶³

In addition to annealing that changes the hydrophilicity of TiO₂ nanotubes (contact angle value decreased from 24.62 ± 5.23 to $10.76 \pm 2.35^\circ$), aging also influences the hydrophobicity properties of TiO₂ nanotubes. Due to the formation of Ti(OH)₄, instead of TiO₂, after anodizing titanium in an electrolyte based on ethylene glycol, the hydrophobicity properties of both as-formed and annealed titania nanotubes increased after 92 days of aging; the contact angle value increased from 24° to 42° and from 10° to 27° for the as-formed and annealed nanotubes, respectively.⁶⁵ It can be deduced that after transferring to a more stable state of TiO₂ after aging, Ti(OH)₄ becomes more hydrophobic.⁶⁵ The viability, proliferation of MC3T3-E1 preosteoblasts, and mineralization on a mixture of anatase and rutile crystallite were higher and more regular than on anatase only and the structure was amorphous.⁶³

As anatase TiO₂ is more biocompatible than amorphous TiO₂, the adhesion, ALP activity and mineralization of MC3T3-E1 preosteoblast were investigated on titania nanotubes with a diameter ranging from 20 to 120 nm and a length of 100 to 400 nm. SEM images of extended MC3T3-E1 preosteoblast cell filopodia on nanotube layers with different diameters are shown in Figure 5: (a) 20 nm, (b) 50 nm, (c) 70 nm, (d) 100 nm, (e) 120 nm ($\times 70,000$), and (f) 120 nm ($\times 30,000$) (reproduced from Yu et al.⁶⁶). Despite the increase in cell proliferation with increases in diameter, there was no other cell behavior observed for nanotubes with a diameter of 70 nm and greater.⁶⁶ It has been proposed that this phenomenon is related to the effect of length and roughness of the nanotubes and to the sensitivity of the filopodia of the cells to the anatase structure.⁶⁶ The crystalline form of TiO₂ nanotubes showed a lower

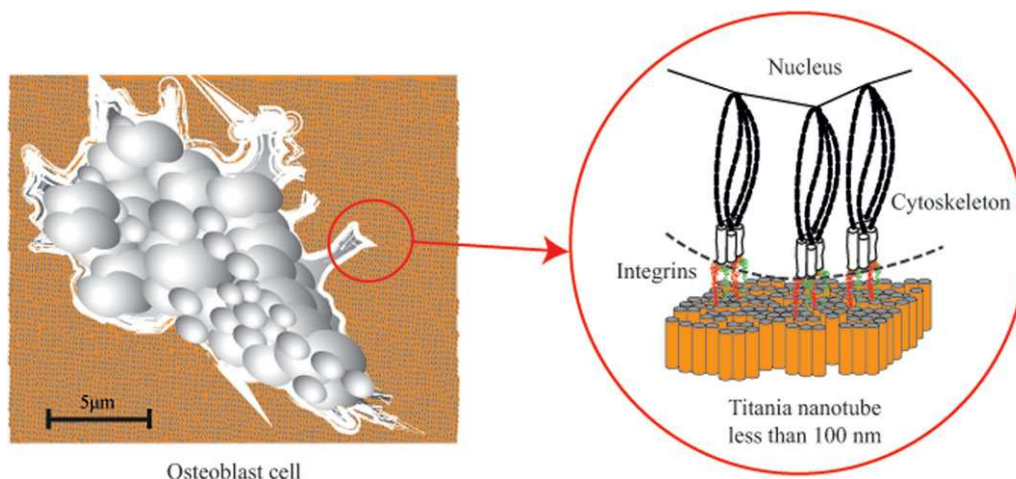


FIGURE 4. Schematic illustration of a bone cell (osteoblast) attached on titania nanotubes with a diameter less than 100 nm (Adapted from Refs. 26 and 87, with permission from J Med Mater Res A and Cell Tissue Res). [Color figure can be viewed in the online issue, which is available at wileyonlinelibrary.com.]

tendency to corrosion in Hank's solution in comparison to the amorphous phase, due to the thicker layer of oxide at the interface of the metal surface and the bottoms of the nanotubes⁶² and it has been demonstrated that annealing helps to stabilize the surface of nanotubes, leading to a higher corrosion resistance.⁶⁴

Effect of HA coating on the surface of TiO₂ nanotubes on bone cell behavior

A bone-like apatite layer forms on the modified surface of biomaterials after implantation in the body. This has been identified as an indispensable stage for bone bonding. The nanotubular structure of TiO₂ promotes the tailoring of a nanosized apatite structure, which has been shown to improve the bioactivity and osteoblast functions. An increased surface area, and pathways for fluid in between the nanotubes, is the most obvious reasons for such functionality of titania nanotubes.⁶⁷ There are several methods for calcium phosphate or HA deposition using physical and chemical techniques, such as plasma spray,⁶⁸ sputtering,^{69,70} electron beam physical vapor deposition (EB-PVD),⁷¹ electrodeposition,⁷² and simpler method: immersion in a simulated body fluid (SBF) such as a Hank's solution.^{60,73}

A large diameter of 200 nm and a small diameter of 100 nm nanotubes composed of TiO₂, Nb₂O₅, and ZrO₂ formed on the surface of Ti-29Nb-5Zr have been coated by TiN, HA, and HA/TiN using a RF magnetron sputtering system. TiN coating had a columnar shape and was well spread onto the nanotubes, exhibiting a high film nucleation and growth rate compared to the HA-coated surface with their coating particles slightly covered on the tops of the nanotubes and well spread on the surface. Multilayer coating of HA/TiN for 1 h deposition of HA and 5 min deposition of TiN showed an entirely spherical shape and the coatings did not block the nanotube tips which could be an optimum condition for enhance high Ca/P absorption, in comparison to the coatings of HA/TiN for 2 h deposition of HA and 10 min deposition of TiN.⁷⁴ The HA coating made of tooth ash

has been coated on 150 and 100 nm nanotubes on the surface of Ti-xHf by EB-PVD to examine their corrosion behaviors. It has been shown that the diameter of nanotubes decrease with increasing Hf content and HA coating covered the tip of nanotubes in lower content of Hf (Ti-20Hf), in reverse to Ti-40Hf. Good corrosion resistance has been obtained by HA coating on top of nanotubes in comparison to nanotubes without coating.⁵⁹ High corrosion resistant HA coating using EB-PVD on top of nanotubes has been reported on the surface of Ti-30Ta-xZr and Ti-30Nb-xZr alloys; with nearly complete covering on Ti-30Ta-15Zr/Ti-30Nb-15Zr alloys, in comparison to a nonuniformly covering on Ti-30Ta-3Zr/Ti-30Nb-3Zr alloys.⁵⁸ The Ca/P ratio of EB-PVD-coated HA on Ti-35Nb-10Zr alloy after heat treatment at 500°C was around 1.67 and the HA exhibited a of 150 nm.⁷⁵

Uniform flaky and hexagonal columnar calcium phosphate ceramics layer, depending on the pH of the electrolyte (pH = 4, 6 respectively) has been grown on anodized titanium surface with a prealkaline treatment nanotubular oxide layer by electrodeposition. Bond strength of the calcium phosphate crystals with 100–200 nm in diameter and about 2 μm long which have been started to deposit at the bottom of the nanotubes of the oxide was from 16 to 19 MPa, whereas calcium phosphate coating onto a polished nonanodized titanium surface have been easily removed by washing due to its weak bonding and nonuniformity.⁷⁶ In another work⁷⁷ the bond strength between HA and alkaline-treated titania nanotubes that has been deposited by pulse electrodeposition method was from 16 to 44 MPa. The bond strength of the as-deposited HA on nanotubes was low; it increased after alkali treatment and annealing at 450 and 600°C. The ring like structure of sodium titanate that has been formed in alkaline treatment at the neck of nanotubes has played an important role to improve the bond strength of the coating with the substrate alongside with the annealing of the HA. Calcium hydrogen phosphate (CaHPO₄·2H₂O) crystals in nanometer scale precipitated on anodized

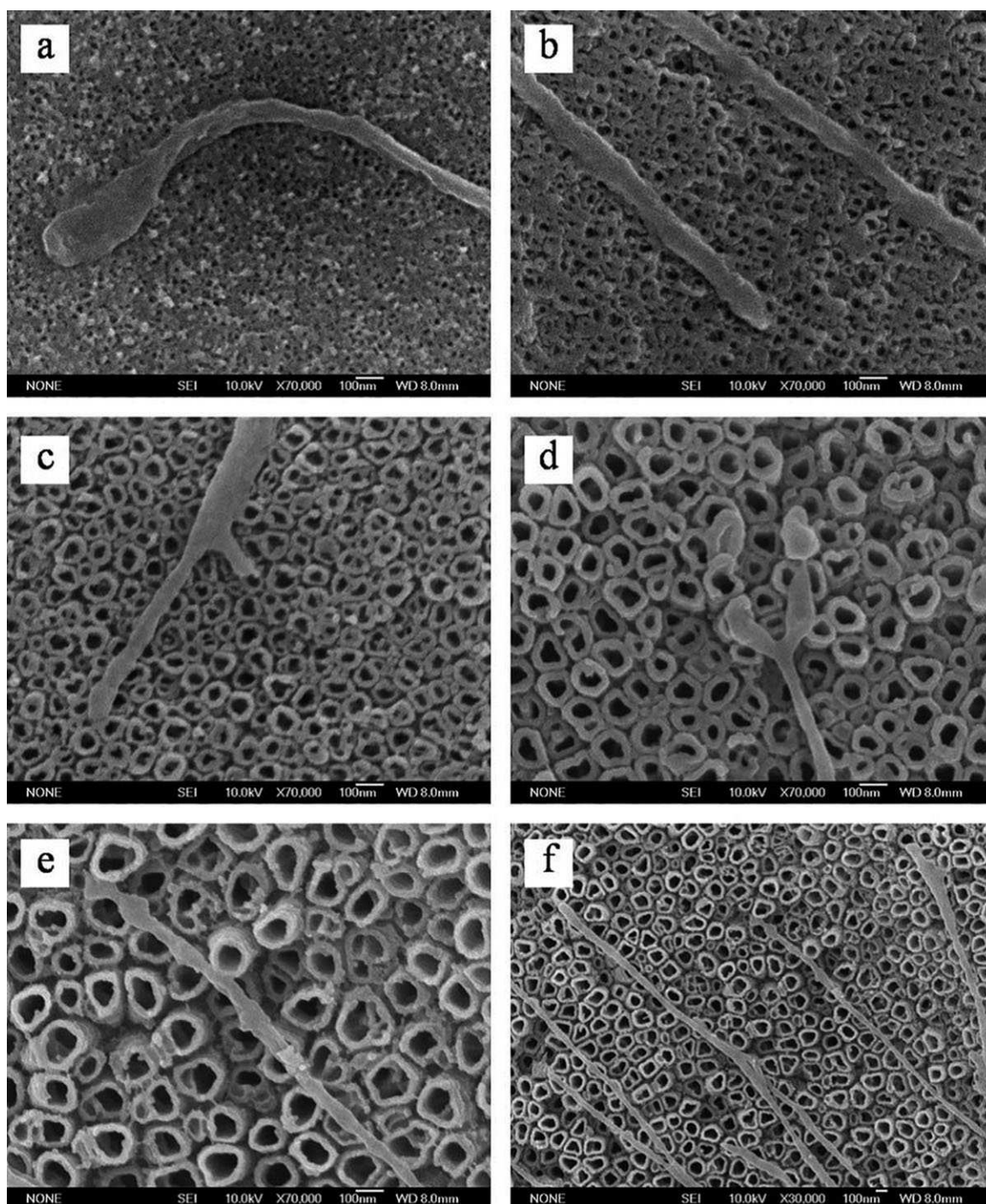


FIGURE 5. SEM images of extended MC3T3-E1 preosteoblast cell filopodia on nanotube layers with different diameters: (a) 20 nm, (b) 50 nm, (c) 70 nm, (d) 100 nm, (e) 120 nm ($\times 70,000$), and (f) 120 nm ($\times 30,000$; Reproduced from Ref. 66, with permission from J Med Mater Res A).

titanium with and without annealing when electrochemically polarized in SBF solution transformed to HA coating in alkaline solution. The bond strength between the HA coating and the substrate was 7.41 MPa because of both the anchoring in and between the tubes, in comparison to Ti without anodic oxidation which exhibited a bond strength of 3.29 MPa.⁷⁸

Calcium phosphate coatings grew uniformly on TiO₂ nanotubes that were 40–110 nm in diameter and about

0.7 μm in length that were annealed at a temperature up to 600°C and immersed in Hank's solution, due to the negative charge nature of titania nanotubes.⁶⁰ The Ca/P ratio of the coating layer after immersion in Hank's solution was 1.16 for 2 days and 1.37 for 7 days, which indicated that the coating layer tended to incorporate more calcium with immersion time. The adsorption of bovine serum albumin (BSA) on a high surface area, such as with a calcium

phosphate coating, increased in comparison to the titanium surface covered with native oxide film, and this enhanced cell adhesion.⁶⁰ An alternative immersion method, preloading the TiO₂ nanotubes with synthetic HA, was used to efficiently deposit synthetic HA, which is affected by pore size and the ion content in the oxide material.⁷³ The Ca/P ratio obtained through this method, which consists of 20 cycles of alternating immersion in a saturated calcium solution followed by 1 min holding time and 1 min washing with ultra-pure water, was about 1.58, which is close to 1.67, the Ca/P ratio of synthetic apatite. The deposition of calcium phosphate on annealed TiO₂ nanotubes increased as the diameter increased from 15 to 100 nm and the length increased from 880 nm to 1.2 μ m.⁷³

Apatite formation differed in terms of the nucleation and growth on the TiO₂ nanotubes, which were formed using two different conditions of stirring electrolyte: (i) a bath stirred using a magnetic pellet and (ii) an ultrasonated bath.⁶⁷ The diameter of titania nanotubes was 75–110 nm with a thickness of 700 nm when formed in an ultrasonated bath and 50–90 nm with a thickness of 900 nm when formed in a magnetically stirred bath. The apatite coatings formed on the larger diameter TiO₂ nanotubes (75–110 nm) after soaking in SBF for 504 h exhibited a smaller crystallite size (15 nm) and a complete covering of the surface; whilst the apatite that formed on smaller diameter nanotubes (50–90 nm) exhibited a larger crystallite size of 25 nm and an islands covering of the surface. The protein activity of MG63 human osteosarcoma cells was higher on the finer apatite coating.⁶⁷ The thickness of the nanotubes showed only an insignificant influence on the cell activity. Meanwhile, HA growth as well as adhesion/proliferation of osteoblasts occurred more effectively on a mixture of anatase and rutile structures, due to annealing, than on anatase only,⁶² although it has been reported that a 10 μ m thick HA coating was formed after 4 days immersion in SBF on the as-formed TiO₂ nanotubes that were treated using several dip-and-dry steps, by which the TiO₂ nanotubes were filled and covered with calcium phosphate nucleation sites.⁷⁹

IN VIVO EFFECT OF MICRO/NANOSTRUCTURE OF THE SURFACE OF TiO₂ NANOTUBES

According to the highly organized hierarchical structures of bone natural tissues that consist of nano-, micro-, and macroscale building blocks⁸⁰ a few attempts have been undertaken to study these phenomena through implantation in the body of selected animals. To translate the role of the micro and nanotopographies on cell functions when primary osteoblasts were seeded on the HF acid-treated/anodized nanotubes substrate, the micro/nanotextured surface topographies showed more biologically friendly rendering, with more balanced promotion in multiple cell functions than the microtopography.⁸¹ The HF acid-treated/anodized nanotubes substrates with screw shape were placed in mandibles of ovariectomized sheep for 12 weeks.⁸² The implant stability quotient values, the maximum pull-out forces, and the bone–implant contact (BIC) have been investigated. Significantly increased bone volume ratio and the trabecular num-

ber with decreasing trabecular separation evidenced the fact that the osseointegration of titanium implant could be improved by a hierarchical micro/nanotextured surface.⁸² In another work⁸³ screw-shaped and anodized titanium implants have been implanted in the femur condyle close to the knee joint of New Zealand white male rabbits. The mean pore size of titania nanotubes was \sim 108 nm, the pore size distribution was \sim 58–150 nm, the porosity was 60%, the roughness (Sa) value was 0.65 (\pm 0.02) μ m and the equivalent values for developed surface area (Sdr) was 14.3% (\pm 0.9). The results of the animal studies based on the osseointegration strengths, new bone formation and bone/cell contact at the bone–implant interface in comparison to the blasted, moderately rough implants demonstrated potential applications of titania nanotubes for bone tissue engineering.⁸³ To examine the effect of the nanotube diameter on cellular activity, five different nanotube diameters (15, 30, 50, 70, and 100 nm) have been implanted in the frontal skull of an adult domestic pig.⁸⁴ The BIC for the 50, 70, and 100 nm groups were greater than control group (untreated) and the bone morphogenetic protein-2 expression within the 50, 70, and 100 nm groups was different. This study showed the important effect of nanotube diameters for the controlled formation of peri-implant bone around medical implant devices. Annealed titania nanotubes with pore size of approximately 80 nm and length of 400 nm have been used to investigate the short- and long-term performance of mesenchymal stem cells *in vitro* and implanted in the scruff region of the neck male Lewis rats *in vivo*.⁸⁵ Higher cell adhesion, proliferation and viability up to 7 days of culture, higher ALP activity and 50% higher calcium and phosphorous concentrations have been observed in comparison to pure titanium and tissue culture polystyrene as a control system with no adverse immune response occurred under *in vivo* conditions.⁸⁵ The *in vitro* outcome of accelerated osteoblast adhesion by \sim 300–400%⁵⁴ of annealed TiO₂ nanotubes has been followed by an investigation of *in vivo* bone bonding in earloop of rabbits for 4 weeks. Bone bonding strength, BIC area, new bone formation, and calcium and phosphorus levels on the nanotube surfaces were increased in comparison to TiO₂ grit-blasted surfaces.⁸⁶ Further studies have to be undertaken to investigate the influence of nanoarchitecture and properties of titanium dioxide nanotubes on bone cell behavior after implantation in the body of animals to confirm the *in vitro* results.

SUMMARY

If bonding between an implant material and bone cannot be formed initially, then acceptance of the implant by the body, or more precisely the bone cell, fails. Titania nanotubes on titanium and titanium alloys (more biocompatible metal implants) can be tailored using anodic oxidation, which is one of the versatile chemical surface treatments. A high surface area, especially the spacing between nanofeatures that is provided by the nanotubes, offers convenient conditions for interlocking with bone cells and the penetration of body fluid. Cells respond to nanoscale structures and nanopatterns and are also sensible to the chemical and mechanical

properties of the surface, such as surface energy, water contact angle and zeta potential. A low contact angle influences cell differentiation and proliferation. Titania nanotubes after annealing existed in a mixture of anatase and rutile, exhibited a more stable morphology, and demonstrated a higher proliferation of MC3T3-E1. A HA layer with a thickness of up to 10 μm on the surface of TiO_2 nanotubes, with different nanotube sizes and forms, can be obtained. In order to establish the optimum nanotopography for cell response, some investigations have been undertaken. The results of *in vitro* studies suggested that the optimum diameter of TiO_2 nanotubes is less than 100 nm and that 15 nm is the best although there are some controversy discussions. If the mechanism of the cell response is clarified, the cell fate at the surface boundary will be more controllable. More studies are needed in order to find the optimum size of nanotubes in length and diameter for the sensing element of a bone cell to be recognized and adhered to and more *in vivo* investigations to confirm the *in vitro* results, especially for the new biocompatible titanium binary, ternary, and quaternary alloys.

REFERENCES

- Niinomi M. Mechanical biocompatibilities of titanium alloys for biomedical applications. *J Mech Behav Biomed Mater* 2008;1(1): 30–42.
- Niinomi M. Metallic biomaterials. *J Artif Organs* 2008;11(3): 105–110.
- Long M, Rack HJ. Titanium alloys in total joint replacement—A materials science perspective. *Biomaterials* 1998;19(18): 1621–1639.
- Navarro M, Michiardi A, Castaño O, Planell JA. Biomaterials in orthopaedics. *J R Soc Interface* 2008;5(27):1137–1158.
- Hench LL, Polak JM. Third-generation biomedical materials. *Science* 2002;295(5557):1014, 1016–1017.
- Liu X, Chu P, Ding C. Surface modification of titanium, titanium alloys, and related materials for biomedical applications. *Mater Sci Eng R* 2004;47(3–4):49–121.
- Zwilling V, Aucouturier M, Darque-Ceretti E. Anodic oxidation of titanium and TA6V alloy in chromic media. An electrochemical approach. *Electrochim Acta* 1999;45:921–929.
- Roy P, Berger S, Schmuki P. TiO_2 nanotubes: Synthesis and applications. *Angew Chem* 2011;50(13):2904–2939.
- Lavenus S, Ricquier JC, Louarn G, Layrolle P. Cell interaction with nanopatterned surface of implants. *Nanomedicine* 2010;5(6): 937–947.
- Anselme K. Osteoblast adhesion on biomaterials. *Biomaterials* 2000;21(7):667–681.
- Brammer KS, Frandsen CJ, Jin S. TiO_2 nanotubes for bone regeneration. *Trends Biotechnol* 2012;30(6):315–322.
- Tan AW, Pingguan-Murphy B, Ahmad R, Akbar SA. Review of titania nanotubes: Fabrication and cellular response. *Ceram Int* 2012; 38(6):4421–4435.
- Anselme K, Ploux L, Ponche A. Cell/material interfaces: Influence of surface chemistry and surface topography on cell adhesion. *J Adhes Sci Technol* 2010;24(5):831–853.
- Finke B, Luethen F, Schroeder K, Mueller PD, Bergemann C, Frant M, Ohl A, Nebe BJ. The effect of positively charged plasma polymerization on initial osteoblastic focal adhesion on titanium surfaces. *Biomaterials* 2007;28(30):4521–4534.
- Lotz MM, Burdsal CA, Erickson HP, McClay DR. Cell adhesion to fibronectin and tenascin: Quantitative measurements of initial binding and subsequent strengthening response. *J Cell Biol* 1989; 109(4):1795–1805.
- Bausch AR, Ziemann F, Boulbitch AA, Jacobson K, Sackmann E. Local measurements of viscoelastic parameters of adherent cell surfaces by magnetic bead microrheometry. *Biophys J* 1998;75(4): 2038–2049.
- Yamamoto A, Mishima S, Maruyama N, Sumita M. A new technique for direct measurement of the shear force necessary to detach a cell from a material. *Biomaterials* 1998;19(7–9):871–879.
- Bowers VM, Fischer LR, Francis GW, Williams KL. A micromechanical technique for monitoring cell–substrate adhesiveness: Measurements of the strength of red blood cell adhesion to glass and polymer test surfaces. *J Biomed Mater Res* 1989;23(12): 1453–1473.
- Truskey GA, Proulx TL. Relationship between 3T3 cell spreading and the strength of adhesion on glass and silane surfaces. *Biomaterials* 1993;14(4):243–254.
- Mege JL, Capo C, Benoliel AM, Bongrand P. Determination of binding strength and kinetics of binding initiation. A model study made on the adhesive properties of P388D1 macrophage-like cells. *Cell Biophys* 1986;8(2):141–160.
- Arvidsson A, Franke-Stenport V, Andersson M, Kjellin P, Sul Y-T, Wennerberg A. Formation of calcium phosphates on titanium implants with four different bioactive surface preparations. An *in vitro* study. *J Mater Sci: Mater Med* 2007;18(10):1945–1954.
- Bruckert F, Weidenhaupt M. Applications of micro- and nanotechnology to study cell adhesion to material surfaces. *J Adhes Sci Technol* 2010;24(13):2127–2140.
- Kabaso D, Gongadze E, Perutková Š, Matschegewski C, Kralj-Iglic V, Beck U, van Rienen U, Iglic A. Mechanics and electrostatics of the interactions between osteoblasts and titanium surface. *Comput Methods Biomech Biomed Eng* 2011;14(5):469–482.
- Decuzzi P, Ferrari M. Modulating cellular adhesion through nanotopography. *Biomaterials* 2010;31(1):173–179.
- Gentile F, Tirinato L, Battista E, Causa F, Liberale C, di Fabrizio EM, Decuzzi P. Cells preferentially grow on rough substrates. *Biomaterials* 2010;31(28):7205–7212.
- Das K, Bose S, Bandyopadhyay A. TiO_2 nanotubes on Ti: Influence of nanoscale morphology on bone cell–materials interaction. *J Biomed Mater Res A* 2009;90A(1):225–237.
- Kim S, Lim J, Lee S, Nam S, Kang H, Choi J. Anodically nanostructured titanium oxides for implant applications. *Electrochim Acta* 2008;53(14):4846–4851.
- Engler AJ, Sen S, Sweeney HL, Discher DE. Matrix elasticity directs stem cell lineage specification. *Cell* 2006;126(4):677–689.
- PelhamJR Jr, Wang YL. Cell locomotion and focal adhesions are regulated by substrate flexibility. *Proc Natl Acad Sci USA* 1997; 94(25):13661–13665.
- Kim TI, Jang JH, Kim HW, Knowles JC, Ku Y. Biomimetic approach to dental implants. *Curr Pharm Des* 2008;14(22): 2201–2211.
- Wang HB, Dembo M, Wang YL. Substrate flexibility regulates growth and apoptosis of normal but not transformed cells. *Am J Physiol Cell Physiol* 2000;279(5):48–545:C1345–C1350.
- Chen G, Wen X, Zhang N. Corrosion resistance and ion dissolution of titanium with different surface microroughness. *Biomed Mater Eng* 1998;8(2):61–74.
- Anselme K, Davidson P, Popa AM, Giazson M, Liley M, Ploux L. The interaction of cells and bacteria with surfaces structured at the nanometre scale. *Acta Biomater* 2010;6(10):3824–3846.
- Jung YL, Donahue HJ. Cell sensing and response to micro- and nanostructured surfaces produced by chemical and topographic patterning. *Tissue Eng* 2007;13(8):1879–1891.
- Lord MS, Foss M, Besenbacher F. Influence of nanoscale surface topography on protein adsorption and cellular response. *Nano Today* 2010;5(1):66–78.
- Li JR, Shi L, Deng Z, Lo SH, Liu GY. Nanostructures of designed geometry and functionality enable regulation of cellular signaling processes. *Biochemistry* 2012;51(30):5876–5893.
- Yim EKF, Leong KW. Significance of synthetic nanostructures in dictating cellular response. *Nanomed Nanotechnol Biol Med* 2005;1(1):10–21.
- Liu X, Chu PK, Ding C. Surface nano-functionalization of biomaterials. *Mater Sci Eng R* 2010;70(3–6):275–302.
- Gulati K, Simovic S, Losic D. Highly ordered titania (TiO_2) nanotube arrays fabricated by electrochemical self-ordering process toward development of implantable drug delivery devices with

- triggered drug release. In: Conference on Optoelectronic and Microelectronic Materials and Devices, COMMAD 2010, Canberra, ACT; 2010. p 159–160.
40. Kim WG, Choe HC. Nanostructure and corrosion behaviors of nanotube formed Ti–Zr alloy. *Trans Nonferr Met Soc China* 2009; 19(4):1005–1008.
41. Jeong Y-H, Lee K, Choe H-C, Ko Y-M, Brantley WA. Nanotube formation and morphology change of Ti alloys containing Hf for dental materials use. *Thin Solid Films* 2009;517(17):5365–5369.
42. Jang SH, Choe HC, Ko YM, Brantley WA. Electrochemical characteristics of nanotubes formed on Ti–Nb alloys. *Thin Solid Films* 2009;517(17):5038–5043.
43. Capellato P, Smith BS, Popat KC, Claro APRA. Fibroblast functionality on novel Ti30Ta nanotube array. *Mater Sci Eng C* 2012;32(7): 2060–2067.
44. Ding D, Ning C, Huang L, Jin F, Hao Y, Bai S, Li Y, Li M, Mao D. Anodic fabrication and bioactivity of Nb-doped TiO₂ nanotubes. *Nanotechnology* 2009;20(30).
45. Choe HC. Nanotubular surface and morphology of Ti-binary and Ti-ternary alloys for biocompatibility. *Thin Solid Films* 2011; 519(15):4652–4657.
46. Li Z, Ning C, Ding D, Liu H, Huang L. Biological properties of Ti–Nb–Zr–O nanostructures grown on Ti35Nb5Zr alloy. *J Nanomater* 2012;12:1–7.
47. Mindroiu M, Pirvu C, Ion R, Demetrescu I. Comparing performance of nanoarchitectures fabricated by Ti6Al7Nb anodizing in two kinds of electrolytes. *Electrochim Acta* 2010;56(1):193–202.
48. Mei S, Zhao L, Wang W, Ma Q, Zhang Y. Biomimetic titanium alloy with sparsely distributed nanotubes could enhance osteoblast functions. *Adv Eng Mater* 2012;14(4):B166–B174.
49. Park J, Bauer S, Von Der Mark K, Schmuki P. Nanosize and vitality: TiO₂ nanotube diameter directs cell fate. *Nano Lett* 2007;7(6): 1686–1691.
50. Von Wilmsowsky C, Bauer S, Lutz R, Meisel M, Neukam FW, Toyoshima T, Schmuki P, Nkenke E, Schlegel KA. In vivo evaluation of anodic TiO₂ nanotubes; an experimental study in the pig. *J Biomed Mater Res B Appl Biomater* 2009;89(1):165–171.
51. Park J, Bauer S, Schlegel KA, Neukam FW, von der Mark K, Schmuki P. TiO₂ nanotube surfaces: 15 nm—An optimal length scale of surface topography for cell adhesion and differentiation. *Small* 2009;5(6):666–671.
52. Brammer KS, Oh S, Cobb CJ, Bjursten LM, Heyde Hvd, Jin S. Improved bone-forming functionality on diameter-controlled TiO₂ nanotube surface. *Acta Biomater* 2009;5(8):3215–3223.
53. Oh S, Brammer KS, Li YSJ, Teng D, Engler AJ, Chien S, Jin S. Reply to Von Der Mark K, Bauer S, Park J, Schmuki P. Looking further into the effects of nanotube dimension on stem cell fate. *Proc Natl Acad Sci USA* 2009;106(24).
54. Oh S, Daraio C, Chen L-H, Pisanic TR, Fiñones RR, Jin S. Significantly accelerated osteoblast cell growth on aligned TiO₂ nanotubes. *J Biomed Mater Res A* 2006;78A(1):97–103.
55. Oh S, Jin S. Titanium oxide nanotubes with controlled morphology for enhanced bone growth. *Mater Sci Eng C* 2006;26(8): 1301–1306.
56. Wang N, Li H, Lü W, Li J, Wang J, Zhang Z, Liu Y. Effects of TiO₂ nanotubes with different diameters on gene expression and osseointegration of implants in minipigs. *Biomaterials* 2011; 32(29):6900–6911.
57. Li Y, Ding D, Ning C, Bai S, Huang L, Li M, Mao D. Thermal stability and in vitro bioactivity of Ti–Al–V–O nanostructures fabricated on Ti6Al4V alloy. *Nanotechnology* 2009;20(6).
58. Choe HC, Kim WG, Jeong YH. Surface characteristics of HA coated Ti–30Ta–xZr and Ti–30Nb–xZr alloys after nanotube formation. *Surf Coat Technol* 2010;205(Suppl 1):S305–S311.
59. Jeong YH, Kim WG, Park GH, Choe HC, Ko YM. Surface characteristics of HA coated Ti–Hf binary alloys after nanotube formation. *Trans Nonferr Met Soc China* 2009;19(4):852–856.
60. Roguska A, Pisarek M, Andrzejczuk M, Dolata M, Lewandowska M, Janik-Czachor M. Characterization of a calcium phosphate–TiO₂ nanotube composite layer for biomedical applications. *Mater Sci Eng C* 2011;31(5):906–914.
61. Varghese OK, Gong D, Paulose M, Grimes CA, Dickey EC. Crystallization and high-temperature structural stability of titanium oxide nanotube arrays. *J Mater Res* 2003;18(1):156–165.
62. Bai Y, Park IS, Park HH, Lee MH, Bae TS, Duncan W, Swain M. The effect of annealing temperatures on surface properties, hydroxyapatite growth and cell behaviors of TiO₂ nanotubes. *Surf Interface Anal* 2011;43(6):998–1005.
63. Yu WQ, Zhang YL, Jiang XQ, Zhang FQ. In vitro behavior of MC3T3-E1 preosteoblast with different annealing temperature titania nanotubes. *Oral Dis* 2010;16(7):624–630.
64. Mazare A, Voicu G, Trusca R, Ionita D. Heat treatment of TiO₂ nanotubes, a way to significantly change their behaviour. *UPB Sci Bull Ser B Chem Mater Sci* 2011;73(1):97–108.
65. Shin DH, Shokuhfar T, Choi CK, Lee SH, Friedrich C. Wettability changes of TiO₂ nanotube surfaces. *Nanotechnology* 2011;22(31).
66. Yu WQ, Jiang XQ, Zhang FQ, Xu L. The effect of anatase TiO₂ nanotube layers on MC3T3-E1 preosteoblast adhesion, proliferation, and differentiation. *J Biomed Mater Res A* 2010;94(4): 1012–1022.
67. Narayanan R, Lee HJ, Kwon TY, Kim KH. Anodic TiO₂ nanotubes from stirred baths: Hydroxyapatite growth & osteoblast responses. *Mater Chem Phys* 2011;125(3):510–517.
68. Khor KA, Dong ZL, Quek CH, Cheang P. Microstructure investigation of plasma sprayed HA/Ti6Al4V composites by TEM. *Mater Sci Eng A* 2000;281(1–2):221–228.
69. Kim WG, Choe HC. Surface characteristics of hydroxyapatite/titanium composite layer on the Ti–35Ta–xZr surface by RF and DC sputtering. *Thin Solid Films* 2011;519(20):7045–7049.
70. Lee K, Choe HC, Kim BH, Ko YM. The biocompatibility of HA thin films deposition on anodized titanium alloys. *Surf Coat Technol* 2010;205(Suppl 1):S267–S270.
71. H-C. Choe, *Surf Coat Technol* 2012; doi:10.1016/j.surfcoat. 2012.05.018.
72. Ma J, Liang CH, Kong LB, Wang C. Colloidal characterization and electrophoretic deposition of hydroxyapatite on titanium substrate. *J Mater Sci: Mater Med* 2003;14(9):797–801.
73. Kodama A, Bauer S, Komatsu A, Asoh H, Ono S, Schmuki P. Bioactivation of titanium surfaces using coatings of TiO₂ nanotubes rapidly pre-loaded with synthetic hydroxyapatite. *Acta Biomater* 2009;5(6):2322–2330.
74. Kim EJ, Jeong YH, Choe HC, Brantley WA. Surface phenomena of HA/TiN coatings on the nanotubular-structured beta Ti–29Nb–5Zr alloy for biomaterials. *Appl Surf Sci* 2012;258(6):2083–2087.
75. Jeong YH, Choe HC, Eun SW. Hydroxyapatite coating on the Ti–35Nb–xZr alloy by electron beam-physical vapor deposition. *Thin Solid Films* 2011;519(20):7050–7056.
76. Raja KS, Misra M, Paramguru K. Deposition of calcium phosphate coating on nanotubular anodized titanium. *Mater Lett* 2005;59(17): 2137–2141.
77. Kar A, Raja KS, Misra M. Electrodeposition of hydroxyapatite onto nanotubular TiO₂ for implant applications. *Surf Coat Technol* 2006;201(6):3723–3731.
78. Wang Y, Tao J, Wang L, He P, Wang T. HA coating on titanium with nanotubular anodized TiO₂ intermediate layer via electrochemical deposition. *Trans Nonferr Met Soc China* 2008;18(3): 631–635.
79. Wang LN, Luo JL. Formation of hydroxyapatite coating on anodic titanium dioxide nanotubes via an efficient dipping treatment. *Metall Mater Trans A* 2011;42(11):3255–3264.
80. Rho JY, Kuhn-Spearing L, Zioupos P. Mechanical properties and the hierarchical structure of bone. *Med Eng Phys* 1998;20(2): 92–102.
81. Zhao L, Mei S, Chu PK, Zhang Y, Wu Z. The influence of hierarchical hybrid micro/nano-textured titanium surface with titania nanotubes on osteoblast functions. *Biomaterials* 2010;31(19): 5072–5082.
82. Xiao J, Zhou H, Zhao L, Sun Y, Guan S, Liu B, Kong L. The effect of hierarchical micro/nanosurface titanium implant on osseointegration in ovariectomized sheep. *Osteoporos Int* 2011;22(6): 1907–1913.
83. Sul YT. Electrochemical growth behavior, surface properties, and enhanced in vivo bone response of TiO₂ nanotubes on

- microstructured surfaces of blasted, screw-shaped titanium implants. *Int J nanomed* 2010;5(1):87–100.
84. Von Wilmowsky C, Bauer S, Roedl S, Neukam FW, Schmuki P, Schlegel KA. The diameter of anodic TiO₂ nanotubes affects bone formation and correlates with the bone morphogenetic protein-2 expression in vivo. *Clin Oral Implants Res* 2012;23(3):359–366.
 85. Papat KC, Leoni L, Grimes CA, Desai TA. Influence of engineered titania nanotubular surfaces on bone cells. *Biomaterials* 2007;28(21):3188–3197.
 86. Bjursten LM, Rasmusson L, Oh S, Smith GC, Brammer KS, Jin S. Titanium dioxide nanotubes enhance bone bonding in vivo. *J Biomed Mater Res A* 2010;92(3):1218–1224.
 87. Mark K, Park J, Bauer S, Schmuki P. Nanoscale engineering of biomimetic surfaces: Cues from the extracellular matrix. *Cell Tissue Res* 2009;339(1):131–153.
 88. Wheeless CR. *Wheeless' Textbook of Orthopaedics* Maryland;1996.
 89. Anselme K. Biomaterials and interface with bone. *Osteoporos Int* 2011;22(6):2037–2042.
 90. Oh S, Brammer KS, Li YSJ, Teng D, Engler AJ, Chien S, Jin S. Stem cell fate dictated solely by altered nanotube dimension. *Proc Natl Acad Sci* 2009;106(7):2130–2135.
 91. Papat KC, Eltgroth M, LaTempa TJ, Grimes CA, Desai TA. Decreased *Staphylococcus epidermis* adhesion and increased osteoblast functionality on antibiotic-loaded titania nanotubes. *Biomaterials* 2007;28(32):4880–4888.
 92. Feng B, Chu X, Chen J, Wang J, Lu X, Weng J. Hydroxyapatite coating on titanium surface with titania nanotube layer and its bond strength to substrate. *J Porous Mater* 2009;17(4):453–458.